Published in final edited form as:
Mol Cancer Ther. 2014 September ; 13(9): 2149–2158. doi:10.1158/1535-7163.MCT-14-0085.

Direct Inhibition of Choline Kinase by a Near-Infrared Fluorescent Carbocyanine

Sean P. Arlauckas, **Anatoliy V. Popov**, and **Edward J. Delikatny***
Department of Radiology, 317 Anatomy-Chemistry Building, 3620 Hamilton Walk, University of Pennsylvania, Philadelphia, PA 19104, USA

Abstract

Choline kinase alpha (ChoK) expression is increasingly being recognized as an important indicator of breast cancer prognosis, however previous efforts to non-invasively measure ChoK status have been complicated by the spectral limitations of *in vivo* magnetic resonance spectroscopy (MRS) and the complex network of enzymes involved in choline metabolism. The most effective ChoK inhibitors are symmetric and contain quaternary ammonium groups within heterocyclic head groups connected by an aliphatic spacer. Characterization of these bis-pyridinium and bis-quinolinium compounds has led to Phase I clinical trials to assess small molecule inhibitors of ChoK for solid tumor treatment. We report the development of a novel carbocyanine dye, JAS239, whose bis-indolium structure conforms to the parameters established for ChoK specificity and whose spacer length confers fluorescence in the near-infrared window. Fluorimetry and confocal microscopy were used to demonstrate that JAS239 rapidly enters breast cancer cells independent of the choline transporters, with accumulation in the cytosolic space where ChoK is active. Radio-tracing and ^{1}H MRS techniques were used to determine that JAS239 binds and competitively inhibits ChoK intracellularly preventing choline phosphorylation while inducing cell death in breast cancer cell lines with similar efficacy to known ChoK inhibitors. Fluorescent molecules that report on ChoK status have potential use as companion diagnostics for non-invasive breast tumor staging, since NIR fluorescence allows for detection of real time probe accumulation *in vivo*. Furthermore, their ability as novel ChoK inhibitors may prove effective against aggressive, therapy-resistant tumors.

Keywords

Choline Kinase; Optical Imaging; Carbocyanine; Breast Cancer; Kinase and Phosphatase Inhibitors

Introduction

Upregulation of Choline kinase alpha (ChoK) has been correlated with histological tumor grade and resistance to anti-estrogen therapies in breast cancer, ultimately indicating a poorer prognosis (1). ChoK catalyzes the conversion of choline to phosphocholine (PC), an

*(E.J.D.) Phone +1-(215)-898-3105. delikatn@mail.med.upenn.edu
The authors disclose no potential conflicts of interest.

important second messenger and the first step in the biosynthesis of the predominant membrane phospholipid, phosphatidylcholine (PtdCho). ChoK activity can be enhanced by a number of clinically-relevant oncogenes (2-4), growth factors (5-7), transcription factors (8, 9), and carcinogens (10) and ChoK overexpression alone is sufficient to induce malignant transformation (4). The nine chemically-equivalent protons in choline yield a strong singlet peak detectable by proton magnetic resonance spectroscopy (^{1}H MRS). MRS studies have found increasing PC and total choline (tCho) levels as breast cell lines progress from normal to immortalized, to oncogene-transformed, to malignant (11). *In vivo* ^{1}H MRS studies have identified choline accumulation in 83% of breast lesions (12). Furthermore, alterations in choline and lipid metabolism detected by MRS are predictive of tumor response to certain therapies (13, 14).

In vivo ^{1}H MRS is limited by spectral resolution, with the tCho peak representing a composite resonance consisting of free choline, PC, and glycerophosphocholine (GPC). Phosphorus (^{31}P) MRS is capable of distinguishing the phosphomonoester PC from the phosphodiester GPC, but ^{31}P-MRS is relatively insensitive requiring large voxels *in vivo*. In addition, direct PC measurements are not always accurate descriptors of ChoK activity due to the catabolic formation of PC by the phospholipase and sphingomyelinase enzymes (Figure 1). There have been efforts to hyperpolarize choline with the intention of monitoring ChoK activity (15, 16), however this approach is limited by the polarization life-time of ^{15}N and has yet to be demonstrated feasible in intact cells or *in vivo* tumor models. Similar strategies utilizing ^{11}C-choline (17) and ^{18}F-choline (18) for positron emission tomography (PET) imaging have been explored but isotope-labeled choline analogs run into the problem of being dependent on the complex families of proteins responsible for choline transport (ChoT: high-affinity choline transporters, choline transporter-like proteins, organic cation transporters, and organic cation/carnitine transporters). Up-regulation of these proteins has been demonstrated in some cancers but their involvement remains, for the most part, poorly understood (19, 20). An alternative method to non-invasively detect ChoK status would be useful to aid in clinical tumor assessment.

ChoK has garnered clinical attention as a biomarker of tumor malignancy, leading to its study as a treatment target. Silencing ChoK via RNAi has been shown to reduce cell proliferation (21), enhance the sensitivity of aggressive cell lines to 5-fluorouracil (22), and reduce tumor growth rates (23) in breast cancer models. The choline mimetic, hemicholinium-3 (HC-3), has long been known to inhibit ChoK, but also interrupts neuronal choline transport and acetylcholinesterase activity (24). Its neurotoxicity at doses relevant for ChoK inhibition (25) led to the development of molecules capable of blocking choline phosphorylation without causing respiratory paralysis (26). The most potent and specific ChoK inhibitors to date have been established by the Lacal lab based on quantitative structure-activity relationship studies of bis-pyridinium (27) and bis-quinolinium (28) HC-3 mimetics (Figure 2). These studies found that lipophilicity enhances anti-proliferative activity but must be optimized due to trade-offs in solubility. The top candidates identified were symmetric and featured two aromatic heterocyclic head-groups, containing quaternary ammonium elements, attached by a linker of optimized length (29). Many of the bis-pyridinium and bis-quinolinium structures feature electron-donating functional groups, which stabilize the positive charge and increase activity (27). Effective inhibitors have been

identified from compounds with aromatic or aliphatic linkers, which can be used to optimize the anti-proliferative properties.

1,1′-((Butane-1,4-diylbis(4,1-phenylene))bis(methylene)) bis(4-(dimethylamino)pyridin-1-ium) bromide (MN58b) is the best-characterized bis-pyridinium ChoK inhibitor, having been demonstrated to be effective against breast, colon (23), bladder (30), and cervical cancer, as well as squamous cell carcinoma, histiocytic lymphoma, and chronic myeloid leukemia models (31). As part of their transformation, cancer cells are thought to build an addiction to PC, which sensitizes them to ChoK-targeted inhibition. MN58b treatment causes a temporary cell cycle arrest in normal cells due to dephosphorylation of the checkpoint protein pRb. This cue for growth arrest is not seen in tumor cells, which attempt to bypass the Kennedy pathway by excising the PC group from sphingomyelin for further PtdCho production, releasing ceramides as a by-product (32). The accumulation of ceramides, in addition to attenuation of the proliferative PC signal, leads to tumor-specific apoptosis (33). TCD-717, developed by TCD Pharma, is the best candidate among the bis-quinolinium compounds and has entered Phase I clinical trials for solid tumor treatment (34).

We sought to test the hypothesis that carbocyanine-derived HC-3 mimetics could be adapted to the established confines for effective ChoK inhibition (Figure 2). The carbocyanine dyes contain a number of structural similarities to existing ChoK inhibitors, including symmetric heterocyclic head-groups containing quaternary ammonium moieties connected by an aliphatic spacer. We report here a new prototype ChoK inhibitor with both potent anti-proliferative activity as well as fluorescence in the near-infrared (NIR) range. The optical properties of NIR fluorophores are ideal for *in vivo* optical imaging, as human tissue (water, hemoglobin, fat) has minimal absorbance in this wavelength range (∼650 - 900 nm). Although fluorescent kinase inhibitors in the visible range have been reported (35-37), our approach using NIR fluorophores potentially allows for the imaging of kinase expression and function *in vivo*.

Materials and Methods

Chemistry Methods

^{1}H NMR spectra were recorded on a Bruker DMX360 or UNI500 spectrometer in $CDCl_3$ or CD_3OD using tetramethylsilane (TMS) as an internal standard. Chemical shifts are reported in ppm. Mass spectra were recorded on a Bruker Microflex MALDI-TOF spectrometer. HPLC analysis was performed as described elsewhere (38). Solvents were purchased from Fisher Scientific. 1,4-Diphenylbutane was purchased from Pfaltz & Bauer, Inc., Waterbury, CT. All other chemicals were purchased from Sigma-Aldrich and used as received. The compounds were named with ChemBioDraw Ultra (v. 13, CambridgeSoft).

Chemical Synthesis

1,4-Bis(4-bromomethylphenyl)butane—1,4-Diphenylbutane (2 g, 9.51 mmol) was added to a mixture of 48% aqueous HBr (4.15 mL, 39.9 mmol) and glacial AcOH (50 mL), followed by 1,3,5-trioxane (0.57 g, 6.34 mmol) and hexadecyltrimethylammonium bromide

(52 mg, 0.143 mmol). The mixture was stirred such that only a single layer could be seen then heated to a gentle reflux for 8 h. The volatiles were removed under reduced pressure. The product was isolated by column chromatography (silica gel, hexane/benzene 1/1, v/v). The isolated 1,4-bis(4-bromomethylphenyl)-butane (1.959 g, yield 52%) was a white solid, mp 119-121 °C (from acetone). ^{1}H NMR (500 MHz, $CDCl_3$, δ ppm) 7.04 ppm (AB, A= 7.18, B= 6.89, J_{AB}= 9 Hz, 8H), 4.53 (s, 4H), 2.66 (m, 4H), 1.62 (m, 4H).

1,1′-((butane-1,4-diylbis(4,1-phenylene))bis(methylene))bis(4-(dimethylamino)pyridin-1-ium) bromide (MN58b)—The mixture of 4-dimethylaminopyridine (238.0 mg, 1.948 mmol) and 1,4-bis(4-bromomethylphenyl)butane (385.9 mg, 0.974 mmol) in dry ethanol (30 mL) was heated and stirred at 160 °C in a 45 mL Parr autoclave equipped with a magnetic stirring bar for 3 h. The white solid product was precipitated twice from EtOH into Et_2O, dissolved in deionized water and lyophilized. Yield: 96%, mp 103-106 °C (from water). ^{1}HNMR (360 MHz, CD_3OD-, δ ppm): 8.21(dt, J = 7.6 Hz, J = 2.9 Hz, 4H, H-2pyr), 7.29 (dm, J = 7.9 Hz, 4H, Ph), 7.23(dm, J = 7.9 Hz, 4H, Ph), 7.00(dm, J = 7.6 Hz, 4H, H-3 pyr), 5.33(s, 4H, C*H*$_2$N$^+$), 3.25(s, 12H, N(C*H*$_3$)$_2$), 2.64(m, 4H, C*H*$_2$C$_6$H$_4$), 1.62(m, 4H, C–C*H*$_2$–C).

1-(2-Hydroxyethyl)-2,3,3-trimethyl-3*H*-indol-1-ium chloride—The mixture of 2,3,3-trimethyl-3H-indole (1592.3 mg, 10 mmol) and 2-chloroethan-1-ol (1610.2 mg, 20 mmol) in dry ethanol (15 mL) was heated and stirred at 160 °C in a 45 mL Parr autoclave equipped with a magnetic stirring bar for 4 h. The purple solid product was precipitated twice from EtOH with Et_2O. Yield 86 %. ^{1}H NMR (360 MHz, CD_3OD, δ ppm): 7.88 ppm (m, 1H); 7.77 (m, 1H); 7.65 (m, 2H); 4.68 (m, 2H); 4.06 (m, 2H); 1.63 (s, 6H); labile OH and N=C-CH_3 protons are in exchange with CD_3OD. MALDI-TOF, m/z: (M-Cl)$^+$ 204.35, calculated for $C_{13}H_{18}NO$ 204.14.

1-(2-hydroxyethyl)-2-((1*E*,3*E*,5*E*)-7-((*Z*/*E*)-1-(2-hydroxyethyl)-3,3-dimethylindolin-2-ylidene)hepta-1,3,5-trien-1-yl)-3,3-dimethyl-3*H*-indol-1-ium chloride (JAS239)—A solution of acetic anhydride (112.3 mg, 1.1 mmol) in CH_2Cl_2 (2 mL) was added to a cooled (-20 °C), stirred suspension of *N*-((1*E*,3*E*,5*Z*)-5-(phenylimino)penta-1,3-dien-1-yl) benzenaminium chloride (142.4 mg, 0.5 mmol) and triethylamine (222.6 mg, 2.2 mmol) in CH_2Cl_2 (10 mL). The resulting clear solution was stirred for another 3 h at room temperature (RT) and concentrated under high vacuum. The residue containing *N*-phenyl-*N*-((1*E*,3*E*,5*Z*)-5-(phenylimino)penta-1,3-dien-1-yl)acetamide was dissolved in ethanol (5.0 mL) and added drop-wise to a refluxing solution of 1-(2-hydroxyethyl)-2,3,3-trimethyl-3*H*-indol-1-ium chloride (360.0 mg, 1.5 mmol) and anhydrous sodium acetate (200 mg, 2.5 mmol) in ethanol (100 mL). The mixture was refluxed for 5 h and concentrated. The product JAS239 was isolated by column chromatography (silica gel, ethyl acetate-methanol (0 - 100%)). Yield 19.9%.^{1}HNMR (360 MHz, CD_3OD, δ ppm): 7.93 (t (dd), J = 13.1 Hz, 2H); 7.58 (t (dd), J = 12.8 Hz, 1H); 7.46 (d, J = 7.2 Hz, 2H); 7.38 (td, J = 7.4 Hz, J = 1.1 Hz, 2H); 7.29 (d, J = 7.9 Hz, 2H); 7.23 (td, J = 7.2 Hz, J = 0.7 Hz, 2H); 6.53 (t (dd), J = 12.6 Hz, 2H); 6.35 (d, J = 13.7 Hz, 2H); 4.21 (t, J = 5.8 Hz, 4H); 4.92 (t, J = 5.8 Hz, 4H); 1.70 (s, 12H). MALDI-TOF, m/z: (M-Cl)$^+$ 469.56, calculated for $C_{31}H_{37}N_2O_2$ 469.28. HPLC: one peak retention time = 15.22 min.

Cell Cultures

Triple-negative human-derived breast cancer MDA-MB-231 cells (ATCC, Manassas, VA, USA) were maintained in DMEM (Mediatech, Manassas, VA, USA) supplemented with 10% FBS (HyClone Laboratories, South Logan, UT, USA), 1% penicillin/streptomycin (Mediatech), and 1% L-glutamine (Mediatech) at 37 °C in a humidified atmosphere (5% CO_2). Genetically-modified MCF-7 breast cancer cells overexpressing ChoKα were provided by Zaver Bhujwalla and Tariq Shah of Johns Hopkins University; further information on the design and characterization of the empty vector (MCF-7 EV) and Chk-4 clone (MCF-7 CK+) transfected cell lines is available in their original publication (39). These cells were cultured in MEM (Mediatech) supplemented with 10% FBS, 1% penicillin/streptomycin, 1% L-glutamine, and 400 mg/ml G418 Sulfate selection agent (Mediatech). G418 was not included in the culture medium during experiments. All cell lines used were tested regularly for mycoplasma. Cells received from ATCC in November of 2011 were used within six months of resuscitation, and authorized by the cell bank via the COI assay, STR analysis, and BacT/ALERT 3D. Cells received from the Bhujwalla lab were tested for mycoplasma upon receipt in March of 2012. Western blots were used to establish the overexpression of ChoKα. Cells were frozen in liquid nitrogen and only used at low passage numbers.

^{14}C-Choline ChoK Activity Assay

Cells were plated at 1.5×10^6 cells/well in 6-well dishes and allowed to grow for 48 h. Media was aspirated and replaced with fresh media containing varying concentrations of MN58B, JAS239, or ethanol control, followed 1 h later by treatment with 0.5 μCi/mL of [methyl-^{14}C]-choline chloride (Perkin Elmer, Santa Clara, CA, USA). At the indicated time-points, cells were rinsed with ice-cold PBS (Mediatech) and fixed in 16% trichloroacetic acid. Samples were scraped, collected in centrifuge tubes, washed 3× in diethyl ether, lyophilized, and resuspended in water for TLC separation using a solvent system of 0.9% NaCl:methanol:ammonium hydroxide (50:70:5; v:v:v). Quantification of the water-soluble choline metabolites was performed using autoradiography with a FujiFilm FLA-7000 in accordance with previously established protocols (31). The R_f values for the choline metabolites were ^{14}C-choline (0.07), ^{14}C-PC (0.14) and ^{14}C-GPC (0.39). In highly-metastatic MDA-MB-231 cells which have high constitutive ChoK expression (21), it takes approximately 17 h for ^{14}C-choline to pass through the Kennedy pathway and be recycled by PLA enzymes to become detectable as ^{14}C-GPC.

Cell viability studies

Cells were plated at 1.5×10^6 cells/well in 6-well plates and incubated for 2 days. Media was removed and replaced with fresh media containing MN58Bor JAS239 at varying concentrations. At the indicated time, cells were rinsed, trypsinized, resuspended in fresh media containing Trypan Blue, and counted using a Neubauer hemacytometer.

^{1}H MRS studies of cellular extracts

MCF-7 cells ($\sim 30 \times 10^6$) were harvested using trypsin and washed 2× with PBS. Dual-phase methanol/chloroform/water extraction was performed in a glass centrifuge tube as

described elsewhere (40) and the aqueous phase roto-evaporated, lyophilized, and resuspended in D_2O containing 0.7 μmole of trimethylsilyl propionate (Aldrich) as standard. Fully relaxed ^1H NMR spectra were acquired using an 11.7 T Varian INOVA high resolution NMR spectrometer and a 90° pulse width (relaxation delay: 6 s; repetition time: 10.73 s; number of scans: 64; data size: 32 K; spectral width: 6000 Hz; temp: 30 °C; total acquisition time: 11 min 28 sec). Spectra were analyzed using Mnova Lite 5.2.5 software with 0.5 Hz apodization. The choline (3.20 ppm), PC (3.22 ppm), and GPC (3.23 ppm) peaks were integrated and compared to TSP (0.00 ppm) values for quantification.

ChoK activity ^1H MRS assay

MCF-7 cells (~20×10^6) were trypsinized, washed 2× in ice-cold PBS, and homogenized on ice in 4 volumes of 100 mM Tris-HCl (pH 8.0) containing 10 mM DTT and 1 mM EDTA in D_2O as described previously (41). Samples were ultrasonicated 2× for 30 sec at 4°C, centrifuged for 30 min, and the supernatant transferred to an NMR tube. ATP (Sigma-Aldrich, St. Louis, MO, USA), choline chloride (Sigma-Aldrich), and $MgCl_2$ (Sigma-Aldrich) in Tris-HCl/D_2O buffer were added to the sample with final concentrations of 10 mM, 2.5 mM, and 10 mM, respectively. ^1H MR spectra were recorded immediately at 10 min intervals for 500 min, (90° pulse length, relaxation delay: 6.6 s; repetition time 10 s; number of scans: 60; data size: 16 K; spectral width: 6000 Hz; temp: 30 °C; total acquisition time: 2 h). Choline and PC peaks were fit from Fourier transformed spectra using Mnova Lite 5.2.5. Data were fit to the linear equation, $y= mx + b$, where x is time, y is the area of the PC or Cho peak, and m, the slope, gives the rate of conversion. To reduce the amount of JAS239 required to treat 20×10^6 cells (grown in 4 150 cm^2 flasks containing 25 mL media each), treatment occurred after cells were pooled and centrifuged, thus 53 nmol of JAS239 were present in the 530 μL NMR sample, equivalent to a concentration of 530 nM if treatment were applied to the cells before trypsinization.

Immunoblot of cell extracts

MCF-7 EV and CK cells were plated in 10 cm dishes (1.0×10^6 cells) and grown for 24 h. Proteins were extracted on ice using radioimmunoprecipitation lysis buffer (Abcam, Cambridge, MA) fortified with a cOmplete Mini, EDTA-free protease inhibitor cocktail (Roche, Mannheim, Germany) and quantified using the BCA Protein Assay Kit (Pierce, Rockford, IL). Approximately 30 μg total protein was resolved on a 10% SDS-PAGE gel, transferred to a nitrocellulose membrane, blocked using non-fat milk, and blotted for ChoKα (Abcam, Cambridge, MA) or GAPDH (Danvers, MA) and imaged using Luminata Western Chemiluminescent HRP substrates (Millipore, Billerica, MA). Bands from each of three separate experiments were quantified using ImageJ software.

Fluorimetry analysis

MDA-MB-231 cells were grown for 48 h in 6-well plates (1.5×10^5 cells/well). Each well was aspirated and replaced with fresh media containing JAS239 with or without choline and incubated for 2 h. Samples were washed in PBS, lysed in DMSO, and the fluorescence measured using a Molecular Devices Spectra Max M5 plate reader (Excitation 640 nm, Emission 770 nm).

Confocal Microscopy

MDA-MB-231 cells were plated at 1.5×10^5 cells/dish in 35 mm glass-bottom dishes coated with poly-D-lysine (MatTek Corp, Ashland, MA, USA). After 2 days of incubation, cells were treated with fresh DMEM containing no phenol red and 2 μM JAS239 and/or 5 μMof the nuclear targeting dye SYTO9 dye (Life Technologies, Carlsbad, CA, USA). The cells were subsequently imaged using a Zeiss LSM 510 META confocal microscope with excitation 633 nm and emission filter 650-790 nm.

Statistics

Data are reported as the mean ± standard deviation (SD) of three separate experiments (n = 3). Probability (p) values were measured using 2-tailed *t*-test; p-values < 0.05 were considered statistically significant.

Results

The structural similarities between the spacered bis-pyridinium/quinolinium ChoK inhibitors and the carbocyanine dyes led us to hypothesize that similar pharmacological activity could exist between the two classes of compounds. To test our hypothesis we designed a carbocyanine dye substituted with choline-like $N^+CH_2CH_2OH$ moieties at the nitrogen atom of the indolinium ring. The synthesis of the carbocyanine precursor, 1-(2-hydroxyethyl)-2,3,3-trimethyl-3*H*-indol-1-ium chloride, was performed in ethanol within an autoclave at high temperature to shorten the reaction time considerably from previous reports in the literature (42). Stable 2-chloroethan-1-ol was used as the alkylating agent, rather than the unstable and more expensive bromo or iodo derivatives, to increase the yield and stability of the intermediates. In the final step we modified a previously reported procedure for the synthesis of C7-carbocyanine (42) to run at a higher temperature by replacing methanol with ethanol as the solvent. This allowed a reduction in the condensation time from 16 h to 5 h (Figure 3A). The reaction can be supervised by colorimetric monitoring as depicted in Figure 3A. The final compound, JAS239, demonstrated NIR fluorescence, with excitation maximum at 740 nm and emission at 770 nm.

To compare the two classes of compounds, we synthesized MN58b as a positive control. The synthesis of MN58b has been reported in two papers where it was referred to as Compound 41 (43, 44). In this paper, we include a detailed description of the synthesis of the intermediate 1,4-bis(4-bromomethylphenyl)butane (Figure 3B), which was not provided in the original papers (45, 46) or in either of the papers describing the synthesis of MN58b (43, 44). In addition, we have improved upon the synthesis of MN58b (Figure 3B) by employing an autoclave method following the phase transfer catalyzed bromomethylation (47). This decreases the reaction time from 192 h (44) to 3 hours with 50% yield. The melting point of our MN58b product differs from that in (44), where it is reported as 161-163°C, but is consistent the values of 98-100°Cwhen the compound was crystallized from water (43).

The novel NIR fluorophoreJAS239 was able to inhibit the phosphorylation of ^{14}C-labeled choline in MDA-MB-231 triple-negative breast cancer cells with an IC_{50} of 4.6 μM at 17 h

of treatment, comparable to the IC_{50} of 2.3 μM observed for MN58b (Figure 4A). Treatment with 10 or 20 μM JAS239 for 17 h or longer resulted in a statistically significant reduction in MDA-MB-231 viability as measured by Trypan Blue exclusion (Figure 4B). The anti-proliferative EC_{50} of JAS239 at 24 h is 13.3 μM. Figure 4C shows that the reduction in choline phosphorylation occurred as early as 2 h post-treatment, before any significant loss in cell viability was observed at 10 and 20 μM. By 17 h, significant losses in both ChoK activity and cell viability were found (Figure 4D). Addition of 2 mM exogenous non-labeled choline to MDA-MB-231 cells was able to rescue the inhibition of ChoK by JAS239 (10 μM) whereas 0.2 mM had no effect (Figure 4E). By 17 h, exogenous choline at 0.2 and 2 mM was unable to outcompete JAS239 (Figure 4F).

Poorly-metastatic MCF-7 breast cancer cells overexpressing ChoKα variant-1 (CK+) and their empty vector controls (EV) were analyzed by NMR to assess baseline choline metabolite levels. ^{1}H NMR spectra of the water-soluble fraction of chloroform:methanol:water extracts of MCF-7 cells (Figure 5A) confirms that ChoK over-expression resulted in increased PC levels (Figure 5B) compared to wild-type MCF-7s ($p = 0.006$), while the empty vector had no effect ($p = 0.286$). The NMR spectra of cytosolic preparations of MCF-7 cells in Figure 5C demonstrate the rise in the PC peak (3.22 ppm) at the expense of the choline peak (3.20 ppm) after choline, ATP, and Mg^{2+} ions were added. The PC and choline peak integrals were plotted over time (Figure 5D) and regressions fit to the linear portion of the curve to estimate ChoK activity. In the presence of sub-micromolar concentrations of JAS239, a 26.2% reduction in ChoK activity ($p = 0.02$) was observed in MCF-7 cells (Figure 5E). ChoK overexpressing MCF-7 CK+ cells demonstrated no significant change in ChoK activity ($p = 0.20$) when exposed to the same concentration of JAS239 (Figure 5E). Western blots were used to confirm the increase in ChoKα expression in MCF-CK+ cells. A representative blot from MCF-7 EV and CK cells are shown in Figure 5F.Quantified protein expression levels demonstrate a 2.3-fold increase in ChoKα levels in MCF-CK+ cells.

The uptake of JAS239wasanalyzed by fluorimetry using MDA-MB-231 cells treated for 2 h at varying concentrations. Fluorescence accumulation was linear within the entire therapeutically-relevant dose range (Figure 6A). Addition of exogenous choline did not obstruct the uptake of JAS239 into these cells (Figure 6B). MDA-MB-231 cells treated with JAS239for2 hand stained for 30 min with the nuclear stain SYTO9 were analyzed using fluorescence confocal microscopy. Figures 6C-E show a distinct separation of SYTO9 (Figure 6C) and JAS239 (Figure 6D) fluorescence, indicating that the localization of the novel probe was confined to the cytosolic space, appearing diffusely in the cytoplasm, as well as in punctate perinuclear spots (Figure 6E), indicating possible organelle accumulation.

Discussion

The goal of this study was to develop a NIR fluorescent ChoK inhibitor by exploiting the structural similarities between the existing bis-symmetric inhibitors and the carbocyanine dyes. Taking into consideration the structural properties established by the Lacal group for ChoK-specific inhibition (29), we developed an autoclave method for carbocyanine

synthesis, which successfully reduced the time required to alkylate the ammonium group of the indolium moiety by 11 h. Using this new method, libraries of promising fluorescent agents can now be synthesized and screened for diagnostic and therapeutic applications in cancer models. The recently reported anticancer activity of substituted benzo[*d*]thiazoles (48), which are common terminal moieties (together with 3,3-dimethyl-3*H*-indole and benzo[*d*]oxazole) in carbocyanine dyes represent one such potential application. In the current study, choline-mimetic hydroxyethyl alkyl groups were attached at the ammonium sites within the heterocyclic head groups on either side of a seven-carbon spacer. The 7-carbon spacing is important because it imparts fluorescence in the NIR range, outside the range of autofluorescence. The resulting JAS239built using the carbocyanine template was analyzed as a NIR-fluorescent ChoK inhibitor. We then adapted the autoclave method to establish a rapid and high yield synthesis of MN58b, the most-effective ChoK inhibitor in the literature.

The number and variety of previously-reported ChoK inhibitors suggests that there exists a certain degree of flexibility in the functional groups and spacers which can yield effective candidate therapeutics. The major concerns for analogs of HC-3 *in vivo* are that they 1) will non-specifically target normal tissue, 2) will disrupt choline uptake into normal cells, which can lead to neuronal toxicity, or 3) will be prone to DNA intercalation, resulting in ChoK-independent cell death. The inherent fluorescence of a carbocyanine-based inhibitor greatly simplifies the process of excluding candidates that inhibit ^{14}C-choline phosphorylation, but are not properly delivered to the intended tissue or sub-cellular compartment. The ability to track the cellular uptake of these fluorophores using fluorimetry and confocal microscopy also permits the determination of potential interactions with choline transporters, which could affect the interpretation of the efficacy of ChoK inhibition *in vitro*. This is also important because compounds that inhibit choline transport have been shown to lead to respiratory paralysis in animals. The broad excitation range of JAS239 and its fluorescence in the NIR window wherein breast tissue is relatively transparent makes it possible to study 1) plasma half-life, biodistribution and tumor localization, 2) cellular uptake pathways and kinetics, and 3) subcellular localization by *in vitro* and *ex vivo* microscopy.

Using ^{14}C-choline as a radiotracer, JAS239 was found to inhibit ChoK activity at concentrations comparable to MN58b, as indicated by reduced production of ^{14}C-PC. ChoK inhibition occurred at 2 h before the onset of cell death and was reversible by addition of unlabeled choline, demonstrating that JAS239 acts as a competitive inhibitor. After 17 h choline addition was unable to reverse the effects of JAS239 on choline metabolism, suggesting that irreversible alterations to the Kennedy pathway had already occurred.

A ^{1}H NMR activity assay was used to explore ChoK kinetics in response to a pulse of choline in the presence of excess ATP and Mg^{2+}. Choline depletion in MCF-7 cells was precisely mirrored by increased PC, confirming the inactivation of competing enzymes by the reducing environment of the cell lysis buffer. The enzymatic rate of ChoK determined by this assay (6.25 nmol PC produced/10^6 cells/hr) was consistent with the observation that ^{14}C-choline phosphorylation upon cell entry is nearly instantaneous. Choline phosphorylation was inhibited by JAS239 but could be rescued by ChoK overexpression, thus confirming that ChoK is the primary target of JAS239that leads to the observed

reduction in choline phosphorylation. This assay measures choline phosphorylation in the absence of choline transporters, suggesting that the decrease in PC levels by JAS239 is independent of their action. Moreover, only nanomolar concentrations of this probe were needed to inhibit ChoK in cell lysates, indicating that functional modifications to the probe which lead to increased uptake into intact cells may further improve efficacy.

The uptake of JAS239 into intact MDA-MB-231 cells was analyzed by fluorimetry and was found to be both rapid and linearly proportional to the concentration of probe added; no quenching of signal intensity was observed even when high therapeutic doses were used. JAS239 appears to enter cells independent of the choline transporters, as exogenous choline addition had no effect on probe uptake. The ability to separate ChoK expression from choline uptake is an advantage to using fluorescent ChoK inhibitors. Reported observations made using MRS and PET measure the effects of both choline transport and phosphorlyation together. This approach may yield a companion diagnostic that would aid in identifying patients best suited for ChoK inhibitor-based therapies. The inherent optical properties of this small molecule inhibitor allow for study of subcellular localization by fluorescence confocal microscopy. JAS239 collects in the cytosolic space where ChoK is active (49) and is excluded from the nucleus where DNA intercalation, mutagenesis, and non-specific cell death would otherwise be confounding factors.

Against pure yeast ChoK, the average reported IC_{50}s of the bis-pyridinium and bis-quinolinium ChoK inhibitors were 37.1 μM and 33.9 μM, respectively; the anti-proliferative activities, EC_{50}s, in HT-29 cells were 19.7 μM and 3.7 μM, respectively (27, 28). Although determined in different systems, the measured IC_{50} of 4.6 μM for JAS239 represents potency comparable or better than 85% of the reported bis-pyridinium-based ChoK inhibitors, and 61% of the bis-quinolinium compounds. The EC_{50} values are also comparable, although determined using different assays in cell lines of different tissue origin. The action of JAS239 against MDA-MB-231 cells suggests ChoK inhibition may be an effective strategy in triple-negative breast cancers which are often therapy-resistant. Its potency suggests that further modifications based upon the carbocyanine template, and subsequent structure-activity characterization, may yield compounds highly specific to ChoK.

Our results have indicated that JAS239 enters breast cancer cells independent of the choline transporters and competes with choline at the active site of ChoK. The development of a small molecule kinase inhibitor with NIR-fluorescence confers the ability to non-invasively track the biodistribution of this probe with NIR optical imaging (50), greatly reducing the number of animals required for detailed pharmacokinetics studies. ChoK expression can be up to fifteen-fold higher in malignant compared to non-transformed breast cells (21), thus imaging agents targeted to this biomarker may benefit from substantial signal-to-noise.

We describe here a novel strategy for reporting ChoK expression, which has been clinically-correlated to histological tumor grade and estrogen receptor status in breast cancer. The simplified chemical synthesis and reaction monitoring technique reported here makes possible the production of carbocyanine-based libraries to be screened for ChoK inhibition and accumulation in breast tumors. As the interest in ChoK inhibitors for cancer therapy

expands, these compounds have the unique potential to serve as companion diagnostics to identify patients most likely to benefit from this therapy and to make on-going minimally-invasive evaluations of their response.

Acknowledgments

The MCF-7 cell lines used were generously provided by Dr. Zaver Bhujwalla and Dr. Tariq Shah at Johns Hopkins University. We thank Mansi Shinde of the Pharmacology Graduate Group at the University of Pennsylvania for assistance with molecular biology techniques. ^{1}H-NMR spectra of cell extracts were acquired using the 11.7 T high resolution MR spectrometer at the Small Animal Imaging Facility (SAIF) of the University of Pennsylvania. Confocal microscopy images were taken with assistance from James Hayden of the Wistar Cancer Institute. Mass spectrometry was performed in the Mass Spectrometry Facility of the Department of Chemistry at the University of Pennsylvania.

Research reported in this publication was supported by the NIH R01-CA129176 (E.J. Delikatny), T32-GM8076 (S.P. Arlauckas), F31-CA180328 (S.P. Arlauckas) and DoD Breast Cancer Concept Award BC076631 (E.J. Delikatny)

References

1. Ramirez de Molina A, Gutierrez R, Ramos MA, Silva JM, Silva J, Bonilla F, et al. Increased choline kinase activity in human breast carcinomas: clinical evidence for a potential novel antitumor strategy. Oncogene. 2002; 21:4317–22. [PubMed: 12082619]
2. Bhakoo KK, Williams SR, Florian CL, Land H, Noble MD. Immortalization and transformation are associated with specific alterations in choline metabolism. Cancer Research. 1996; 56:4630–5. [PubMed: 8840976]
3. Ramirez de Molina A, Penalva V, Lucas L, Lacal JC. Regulation of choline kinase activity by Ras proteins involves Ral-GDS and PI3K. Oncogene. 2002; 21:937–46. [PubMed: 11840339]
4. Ramirez de Molina A, Gallego-Ortega D, Sarmentero J, Banez-Coronel M, Martin-Cantalejo Y, Lacal JC. Choline Kinase Is a Novel Oncogene that Potentiates RhoA-Induced Carcinogenesis. Cancer Research. 2005; 65:5647–53. [PubMed: 15994937]
5. Warden CH, Friedkin M. Regulation of phosphatidylcholine biosynthesis by mitogenic growth factors. Biochim Biophys Acta, Lipids Lipid Metab. 1984; 792:270–80.
6. Cuadrado A, Carnero A, Dolfi F, Jimenez B, Lacal JC. Phosphorylcholine - a Novel 2nd Messenger Essential for Mitogenic Activity of Growth-Factors. Oncogene. 1993; 8:2959–68. [PubMed: 8414498]
7. Jimenez B, Delpeso L, Montaner S, Esteve P, Lacal JC. Generation of Phosphorylcholine as an Essential Event in the Activation of Raf-1 and Map-Kinases in Growth Factors-Induced Mitogenic Stimulation. Journal of Cellular Biochemistry. 1995; 57:141–9. [PubMed: 7721953]
8. Aoyama C, Ishidate K, Sugimoto H, Vance DE. Induction of choline kinase alpha by carbon tetrachloride (CCl4) occurs via increased binding of c-jun to an AP-1 element. Biochim Biophys Acta, Mol Cell Biol Lipids. 2007; 1771:1148–55.
9. Glunde K, Shah T, Winnard PT, Raman V, Takagi T, Vesuna F, et al. Hypoxia regulates choline kinase expression through hypoxia-inducible factor-lot signaling in a human prostate cancer model. Cancer Research. 2008; 68:172–80. [PubMed: 18172309]
10. Ishidate K, Tsuruoka M, Nakazawa Y. Induction of Choline Kinase by Polycyclic Aromatic Hydrocarbon Carcinogens in Rat-Liver. Biochemical and Biophysical Research Communications. 1980; 96:946–52. [PubMed: 6252895]
11. Aboagye EO, Bhujwalla ZM. Malignant transformation alters membrane choline phospholipid metabolism of human mammary epithelial cells. Cancer Research. 1999; 59:80–4. [PubMed: 9892190]
12. Katz-Brull R, Lavin PT, Lenkinski RE. Clinical Utility of Proton Magnetic Resonance Spectroscopy in Characterizing Breast Lesions. Journal of the National Cancer Institute. 2002; 94:1197–203. [PubMed: 12189222]

13. Negendank W. Studies of Human Tumors by MRS - a Review. NMR in Biomedicine. 1992; 5:303–24. [PubMed: 1333263]
14. Delikatny EJ, Chawla S, Leung DJ, Poptani H. MR-visible lipids and the tumor microenvironment. NMR in Biomedicine. 2011; 24:592–611. [PubMed: 21538631]
15. Gabellieri C, Reynolds S, Lavie A, Payne GS, Leach MO, Eykyn TR. Therapeutic Target Metabolism Observed Using Hyperpolarized 15N Choline. J Am Chem Soc. 2008; 130:4598–9. [PubMed: 18345678]
16. Sarkar R, Comment A, Vasos PR, Jannin S, Gruetter R, Bodenhausen G, et al. Proton NMR of 15N-Choline Metabolites Enhanced by Dynamic Nuclear Polarization. J Am Chem Soc. 2009; 131:16014–5. [PubMed: 19848401]
17. Contractor K, Challapalli A, Barwick T, Winkler M, Hellawell G, Hazell S, Tomasi G, Al-Nahhas A, Mapelli P, Kenny LM, Tadrous P, Coombes RC, Aboagye EO, Mangar S. Use of [11C]Choline PET-CT as a Noninvasive Method for Detecting Pelvic Lymph Node Status from Prostate Cancer and Relationship with Choline Kinase Expression. Clin Cancer Res. 2011; 17:7673–83. [PubMed: 22038995]
18. Bansal A, Shuyan W, Hara T, Harris RA, DeGrado TR. Biodistribution and metabolism of [18F]fluorocholine in 9L glioma cells and 9L glioma-bearing fisher rats. Eur J Nucl Med Mol Imaging. 2008; 35:1192–203. [PubMed: 18264706]
19. Glunde K, Bhujwalla ZM, Ronen SM. Choline metabolism in malignant transformation. Nat Rev Cancer. 2011; 11:835–48. [PubMed: 22089420]
20. Eliyahu G, Kreizman T, Degani H. Phosphocholine as a biomarker of breast cancer: Molecular and biochemical studies. Int J Cancer. 2007; 120:1721–30. [PubMed: 17236204]
21. Glunde K, Raman V, Mori N, Bhujwalla ZM. RNA interference-mediated choline kinase suppression in breast cancer cells induces differentiation and reduces proliferation. Cancer Research. 2005; 65:11034–43. [PubMed: 16322253]
22. Mori N, Glunde K, Takagi T, Raman V, Bhujwalla ZM. Choline kinase down-regulation increases the effect of 5-fluorouracil in breast cancer cells. Cancer Research. 2007; 67:11284–90. [PubMed: 18056454]
23. Al-Saffar NMS, Troy H, Ramirez de Molina A, Jackson LE, Madhu B, Griffiths JR, et al. Noninvasive magnetic resonance spectroscopic pharmacodynamic markers of the choline kinase inhibitor MN58b in human carcinoma models. Cancer Research. 2006; 66:427–34. [PubMed: 16397258]
24. Ansell GB, Spanner SG. Inhibition of Brain Choline Kinase by Hemicholinium-3. Journal of Neurochemistry. 1974; 22:1153–5. [PubMed: 4369317]
25. Cannon JG. Structure-Activity Aspects of Hemicholinium-3 (HC-3) and Its Analogs and Congeners. Medicinal Research Reviews. 1994; 14:505–31. [PubMed: 7815851]
26. Hernandez-Alcoceba R, Saniger L, Campos J, Nunez MC, Khaless F, Gallo MA, et al. Choline kinase inhibitors as a novel approach for antiproliferative drug design. Oncogene. 1997; 15:2289–301. [PubMed: 9393874]
27. Campos J, del Carmen Nunez M, Rodriguez V, Entrena A, Hernandez-Alcoceba R, Fernandez F, et al. LUMO energy of model compounds of bispyridinium compounds as an index for the inhibition of choline kinase. Eur J Med Chem. 2001; 36:215–25. [PubMed: 11337100]
28. Sanchez-Martin R, Campos JM, Conejo-Garcia A, Cruz-Lopez O, Banez-Coronel M, Rodriguez-Gonzalez A, et al. Symmetrical bis-quinolinium compounds: New human choline kinase inhibitors with antiproliferative activity against the HT-29 cell line. Journal of Medicinal Chemistry. 2005; 48:3354–63. [PubMed: 15857141]
29. Campos JM, Sanchez-Martin RM, Conejo-Garcia A, Entrena A, Gallo MA, Espinosa A. (Q)SAR studies to design new human choline kinase inhibitors as antiproliferative drugs. Current Medicinal Chemistry. 2006; 13:1231–48. [PubMed: 16712467]
30. Hernando E, Sarmentero-Estrada J, Koppie T, Belda-Iniesta C, Ramirez de Molina V, Cejas P, et al. A critical role for choline kinase-alpha in the aggressiveness of bladder carcinomas. Oncogene. 2009; 28:2425–35. [PubMed: 19448670]

31. Hernandez-Alcoceba R, Fernandez F, Lacal JC. In vivo antitumor activity of choline kinase inhibitors: A novel target for anticancer drug discovery. Cancer Research. 1999; 59:3112–8. [PubMed: 10397253]
32. Rodriguez-Gonzalez A, Ramirez de Molina A, Fernandez F, Lacal JC. Choline kinase inhibition induces the increase in ceramides resulting in a highly specific and selective cytotoxic antitumoral strategy as a potential mechanism of action. Oncogene. 2004; 23:8247–59. [PubMed: 15378008]
33. Kolesnick R. The therapeutic potential of modulating the ceramide/sphingomyelin pathway. Journal of Clinical Investigation. 2002; 110:3–8. [PubMed: 12093880]
34. Ramirez de Molina, A.; Garcia Oroz, L.; Lacal Sanjuan, JC. inventors; Translational Cancer Drugs Pharma S.L., Spain assignee. Methods and Compositions for the Treatment of Cancer. US2011/0256241 A1. 2011.
35. Yenugonda VM, Deb TB, Grindrod SC, Dakshanamurthy S, Yang Y, Paige M, et al. Fluorescent cyclin-dependent kinase inhibitors block the proliferation of human breast cancer cells. Bioorganic & Medicinal Chemistry. 2011; 19:2714–25. [PubMed: 21440449]
36. Kim D, Lee H, Jun H, Hong SS, Hong S. Fluorescent phosphoinositide 3-kinase inhibitors suitable for monitoring of intracellular distribution. Bioorganic & Medicinal Chemistry. 2011; 19:2508–16. [PubMed: 21459582]
37. Kim D, Jun H, Lee H, Hong SS, Hong S. Development of New Fluorescent Xanthines as Kinase Inhibitors. Organic Letters. 2010; 12:1212–5. [PubMed: 20184370]
38. Kachur A, Popov A, Karp J, Delikatny EJ. Direct Fluorination of Phenolsulfonphthalein: A Method for Synthesis of Positron-Emitting Indicators for In Vivo pH Measurement. Cell Biochem Biophys. 2013; 66:1–5. [PubMed: 22790882]
39. Shah T, Wildes F, Penet MF, Winnard PT, Glunde K, Artemov D, et al. Choline kinase overexpression increases invasiveness and drug resistance of human breast cancer cells. NMR in Biomedicine. 2010; 23:633–42. [PubMed: 20623626]
40. Tyagi RK, Azrad A, Degani H, Salomon Y. Simultaneous extraction of cellular lipids and water-soluble metabolites: Evaluation by NMR spectroscopy. Magnetic Resonance in Medicine. 1996; 35:194–200. [PubMed: 8622583]
41. Iorio E, Mezzanzanica D, Alberti P, Spadaro F, Ramoni C, D'Ascenzo S, et al. Alterations of choline phospholipid metabolism in ovarian tumor progression. Cancer Research. 2005; 65:9369–76. [PubMed: 16230400]
42. Ye Y, Li WP, Anderson CJ, Kao J, Nikiforovich GV, Achilefu S. Synthesis and Characterization of a Macrocyclic Near-Infrared Optical Scaffold. J Am Chem Soc. 2003; 125:7766–7. [PubMed: 12822971]
43. Campos J, Núñez M, Sánchez RM, Gómez-Vidal JA, Rodriguez-González A, Báñez M, et al. Quantitative structure–activity relationships for a series of symmetrical bisquaternary anticancer compounds. Bioorganic & Medicinal Chemistry. 2002; 10:2215–31. [PubMed: 11983519]
44. Conejo-García A, Pisani L, del Carmen Núñez M, Catto M, Nicolotti O, Leonetti F, et al. Homodimeric Bis-Quaternary Heterocyclic Ammonium Salts as Potent Acetyl- and Butyrylcholinesterase Inhibitors: A Systematic Investigation of the Influence of Linker and Cationic Heads over Affinity and Selectivity. Journal of Medicinal Chemistry. 2011; 54:2627–45. [PubMed: 21417225]
45. Cram DJ, Steinberg H. Macro rings. I. Preparation and spectra of the paracyclophanes. J Am Chem Soc. 1951; 73:5691–704.
46. Goodson JA, Goodwin LJ, Gorvin JH, Goss MD, Kirby KS, Lock JA, et al. Chemotherapy of amebiasis. III. Variants of bis(diamylamino)decane. Br J Pharmacol Chemother. 1948; 3:62–71. [PubMed: 18904725]
47. Mitchell RH, Iyer VS. An improved procedure for bromomethylation of aromatics using phase-transfer catalysis. Rapid bis-haloalkylation. Synlett. 1989:55–7.
48. Luzina EL, Popov AV. Synthesis and anticancer activity of N-bis(trifluoromethyl)alkyl-N′-thiazolyl and N-bis(trifluoromethyl)alkyl-N′-benzothiazolyl ureas. Eur J Med Chem. 2009; 44:4944–53. [PubMed: 19740574]

49. Hosaka K, Murakami T, Kodaki T, Nikawa J, Yamashita S. Repression of choline kinase by inositol and choline in Saccharomyces cerevisiae. Journal of Bacteriology. 1990; 172:2005–12. [PubMed: 2156807]

50. Yang X, Shi C, Tong R, Qian W, Zhau HE, Wang R, et al. Near IR Heptamethine Cyanine Dye–Mediated Cancer Imaging. Clinical Cancer Research. 2010; 16:2833–44. [PubMed: 20410058]

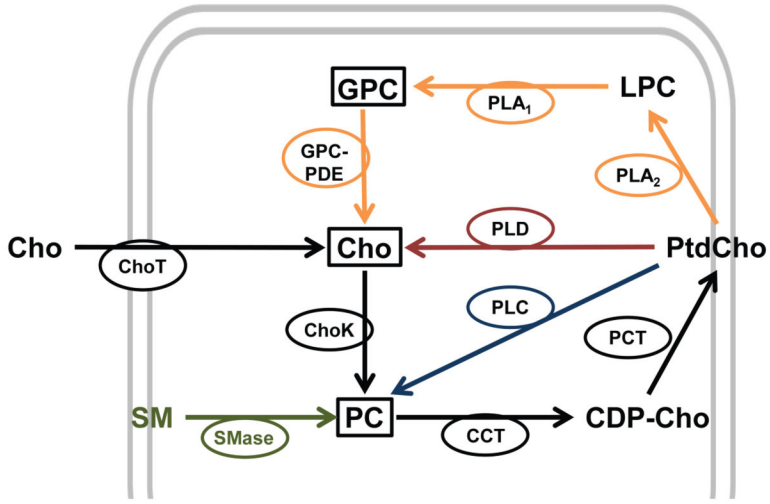

Figure 1.

Mechanisms affecting the intracellular pool of PC: 1) choline (Cho) uptake via Cho transporters (ChoT) and entry into the Kennedy pathway of PtdCho biosynthesis (black) by which Cho is phosphorylated by ChoK (EC 2.7.1.32), then converted to CDP-cho and PtdCho by CHOLINE PHOSPHATE CYTIDYLYLTRANSFERASE (CT; EC 2.7.7.15) and PHOSPHOCHOLINE DIACYLGLYCEROL TRANSFERASE (PCT; EC 2.7.8.2), respectively. The four catabolic routes (dashed lines): 2) membrane sphingomyelin (SM) hydrolyzed by SPHINGOMYELINASE (SMase; EC 3.1.4.12) (green) to PC and ceramide; 3) PtdCho deacylation to lyso-PtdCho (LPC), GPC, and Cho (yellow) by PHOSPHOLIPASE A2 (PLA2; EC 3.1.1.4), and LYSOPHOSPHOLIPASE (EC 3.1.1.5) or PHOSPHOLIPASE A1 (PLA1; EC 3.1.1.32), and GPC:PHOSPHODIESTERASE (GPC:PDE; EC 3.1.4.2), respectively; 4) PtdCho hydrolysis directly to cho and phosphatidic acid by PHOSPHOLIPASE D (PLD; EC 3.1.4.4) (red); 5) PtdCho hydrolysis directly to PC and diacylglycerol via PTDCHO-SPECIFIC PHOSPHOLIPASE C (PLC; EC 3.1.4.3) (blue). ^{1}H MR-visible cho metabolites which contribute to the composite tCho peak are in boxes.

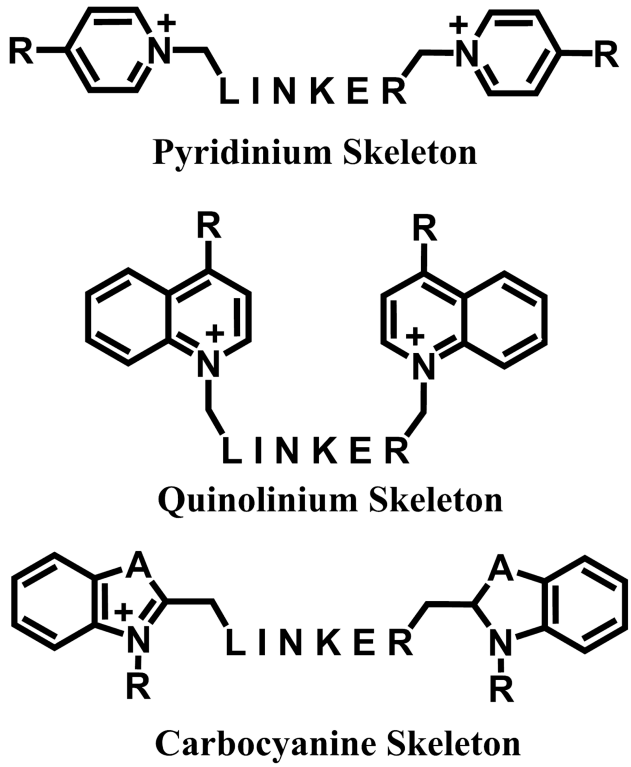

Figure 2.

Templates for ChoK-specific inhibitors: The bis-pyridinium (top) and bis-quinolinium (middle) structures with electron-donating functional groups (R) and aromatic or aliphatic linkers. A novel template for ChoK inhibitors is proposed based upon the carbocyanines (bottom), whose fluorescence properties are determined by linker length and are substitutable at the A and R positions.

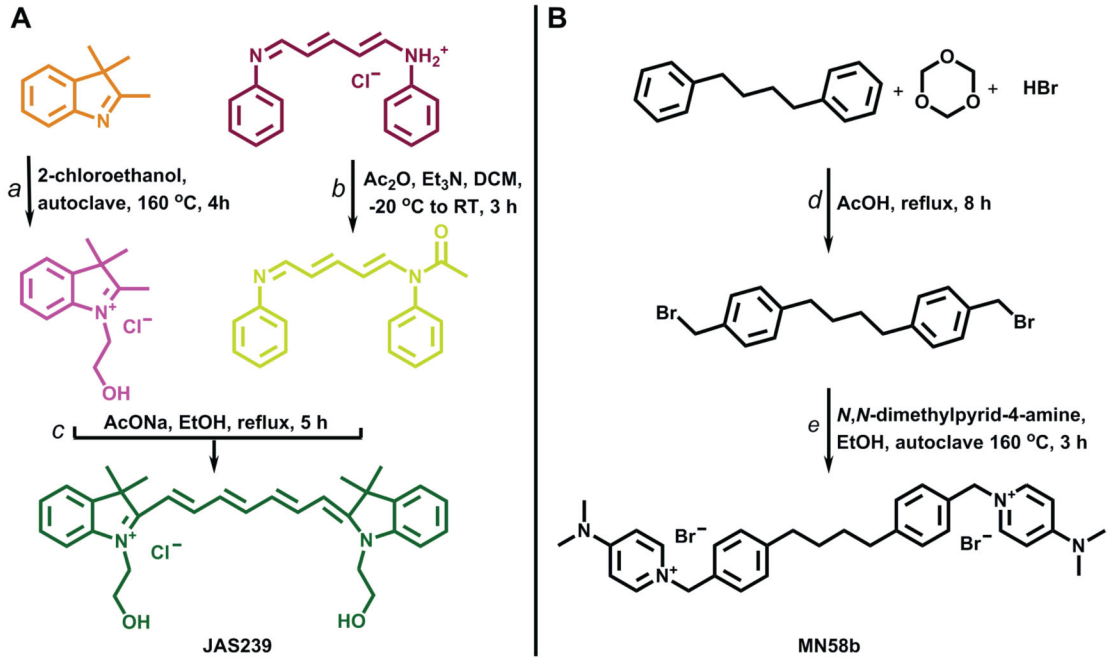

Figure 3.

Synthetic pathway for the preparation of ChoK inhibitors: (A) JAS239 Synthesis: a) 2-chloroethan-1-ol, autoclave 160 °C, 4 h; b) Ac_2O, Et_3N, DCM, -20 °C-RT, 3 h; c) AcONa, EtOH, reflux, 5 h.(B) MN58b Synthesis: d) HBr, cetyltrimethylammonium bromide ($C_{16}H_{33}N(CH_3)_3Br$), acetic acid, reflux, 24 h; e) N,N-dimethylpyridin-4-amine, EtOH, autoclave 160 °C, 3 h.

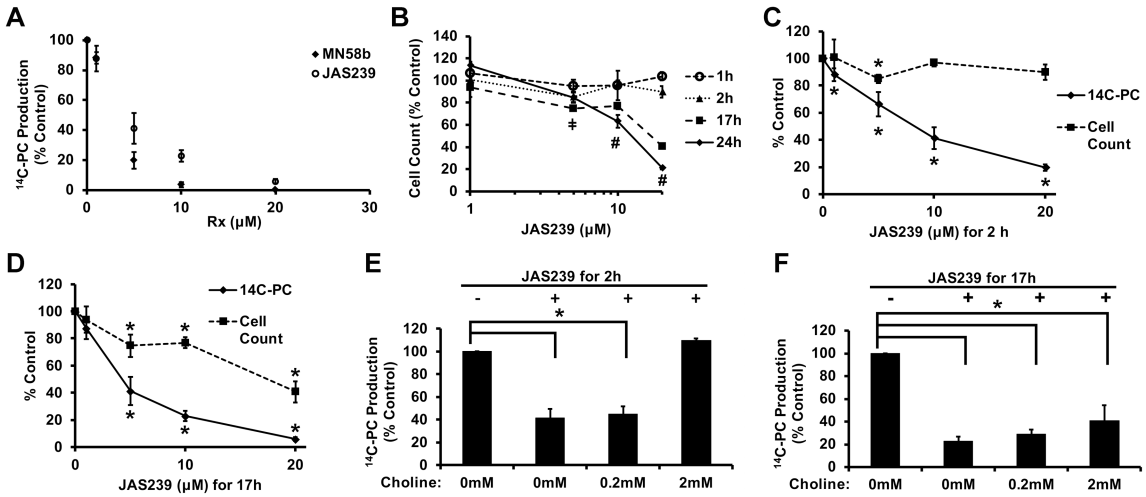

Figure 4.

JAS239 is a competitive inhibitor of ChoK in MDA-MB-231 cells: (A) Cell treatment for 17 h with MN58b or JAS239 inhibits ^{14}C-choline phosphorylation with an IC_{50} of 2.3 and 4.6 μM respectively; (B) Cell viability determined by Trypan blue exclusion in response to JAS239, where ‡ indicates cell reduction ($p < 0.05$) vs untreated control at 2 and 17 h and # indicates cell reduction ($p < 0.05$) vs untreated control at 17 and 24 h; (C) 2 h exposure to JAS239 caused inhibition of ^{14}C-choline phosphorylation with no effect on cell viability; (D) At 17 h exposure to JAS239, both inhibition of ^{14}C-choline phosphorylation and reduction in viability is observed; (E) Exogenous choline addition at high concentrations rescues ^{14}C-choline phosphorylation in cells treated with 10 μM of JAS239 for 2 h; (F) By 17 h, exogenous choline addition does not significantly change ^{14}C-choline phosphorylation in cells treated with 10 μM of JAS239. Data plotted as % control ± SD for 3 separate experiments, *$p < 0.05$.

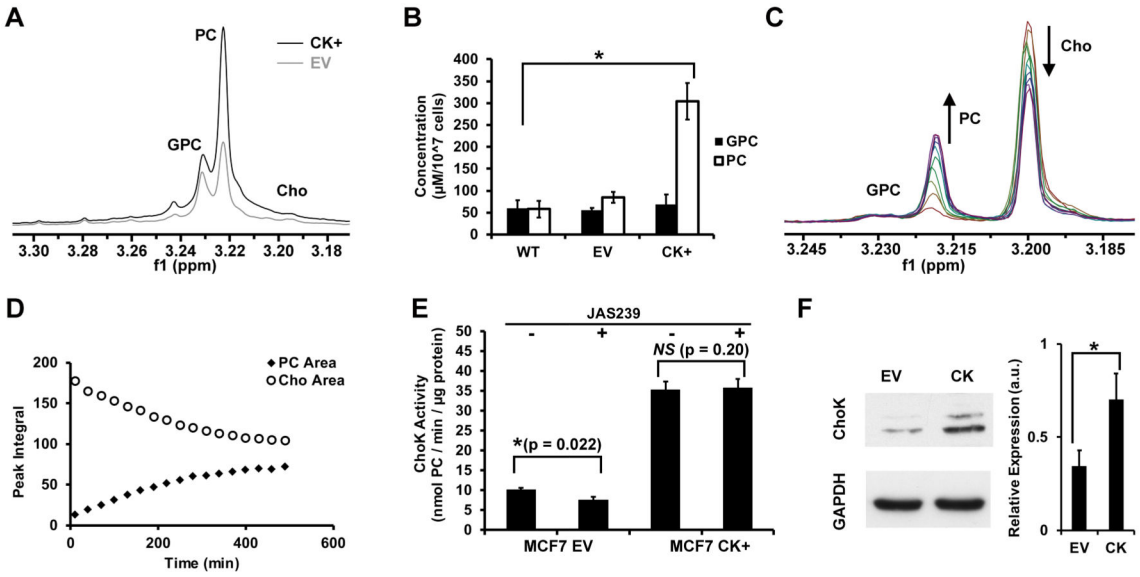

Figure 5.

ChoK inhibition and rescue in ^{1}H NMR assays: (A) Expanded ^{1}H NMR spectra of the aqueous portion of chloroform:methanol:water extracts prepared from ChoKα overexpressing MCF-7s (CK+) or empty vector (EV) control; (B) Concentration-per-cell of NMR-detectable water-soluble choline metabolites in wild-type (WT), empty vector (EV), and ChoKα overexpressing (CK+) MCF-7s; (C) Superimposed ^{1}H spectra obtained over 500 min following addition of choline, Mg^{2+} and ATP to cytosolic extracts of MCF-7 WT cells show increases in PC at the expense of choline; (D) Corresponding PC and Cho peak integrals plotted over time; (E) Regression of the linear portion of (D) yields an estimate of ChoK activity, which is reduced by 530 nM of JAS239 in empty vector (MCF7 EV) cells, but unaffected in overexpressing (MCF7 CK+) cells. (F) Representative immunoblot for ChoKα and GAPDH (loading control) of MCF-7 EV vs. CK cells and the quantified ChoKα/GAPDH expression levels confirming ChoKα overexpression. Error bars represent ± SD for 3 separate experiments, *$p < 0.05$.

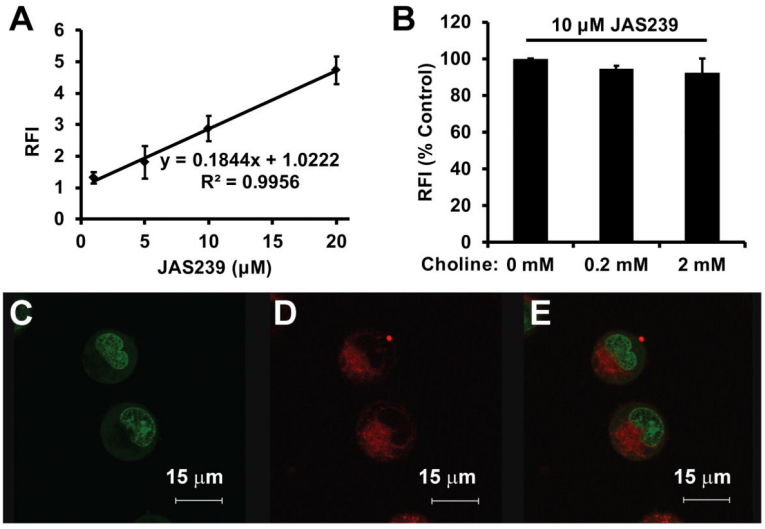

Figure 6.

Uptake and subcellular localization of JAS239: (A) MDA-MB-231 cells treated with varying concentrations of JAS239 for 2 h demonstrate linear increases in relative fluorescence intensity (RFI) (Excitation 640 nm, Emission 770 nm). (B) Fluorimetry study demonstrating that addition of exogenous choline to MDA-MB-231 cells could not outcompete uptake of JAS239; Fluorescence confocal micrographs show MDA-MB-231 cells stained for 30 min with (C) the nuclear stain Syto9, (D) 2 μM of JAS239 and (E) merged images; Error bars represent ± SD for three separate experiments.